Journal of Physics A: Mathematical and Theoretical

PAPER

A study of the ambiguity in the solutions to the Diophantine equation for Chern numbers

To cite this article: J E Avron *et al* 2014 *J. Phys. A: Math. Theor.* **47** 185202

IOP Publishing Journal of Physics A: Mathematical and Theoretical
J. Phys. A: Math. Theor. **47** (2014) 185202 (10pp) doi:10.1088/1751-8113/47/18/185202

A study of the ambiguity in the solutions to the Diophantine equation for Chern numbers

J E Avron[1], **O Kenneth**[1] **and G Yehoshua**[2]

[1] Department of Physics, Technion, Israel Institute of Technology, Haifa, 32000, Israel
[2] Department of Mathematics, Technion, Israel Institute of Technology, Haifa, 32000, Israel

Received 22 September 2013, revised 12 January 2014
Accepted for publication 13 February 2014
Published 22 April 2014

Abstract
The Chern numbers for Hofstadter models with rational flux $2\pi\, p/q$ are partially determined by a Diophantine equation. A mod q ambiguity remains. The resolution of this ambiguity is only known for the rectangular lattice with nearest neighbors hopping where it has the form of a 'window condition'. We study a Hofstadter butterfly on the triangular lattice for which the resolution of ambiguity is open. In the model many pairs (p, q) satisfy a window condition which is shifted relative to the window of the square model. However, we also find pairs (p, q) where the Chern numbers do not belong to *any contiguous window*. This shows that the rectangular model and the one we study on the triangular lattice are not adiabatically connected: many gaps must close. Our results suggest the conjecture that the mod q ambiguity in the Diophantine equation generically reduces to a sign ambiguity.

Keywords: Hofstadter model, quantum Hall phase diagrams, Diophantine equations, window conditions
PACS number: 73.43.−f

(Some figures may appear in color only in the online journal)

1. Motivation and results

Hofstadter models give rise to topological phase diagrams[3] with fractal structure [1, 3]. The phases are labeled by the (integer) Hall conductances (Chern numbers). A high resolution diagram, such as figure 1, requires efficient algorithms for approximating the fractal spectrum of the Hofstadter models as well as an efficient algorithm to compute the Chern numbers that color the wings of the butterfly.

[3] The phase diagrams we consider should be distinguished from phase diagrams which describe the localization properties and the Liapunov exponent described e.g. in [12].

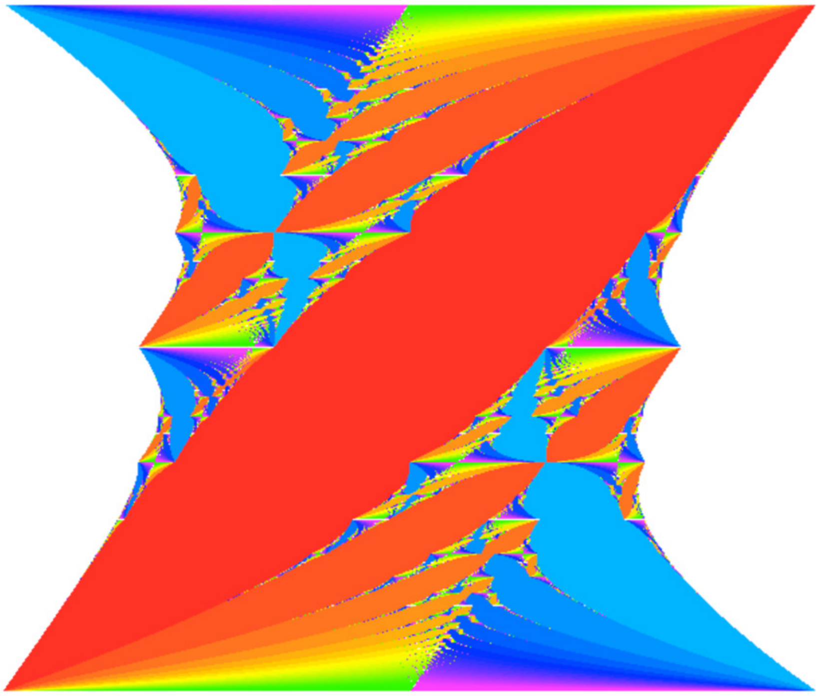

Figure 1. A phase diagram for the Hofstadter model on a triangular lattice where the flux through the down triangle is $\Phi_d = \pi/2$. The vertical axis is the total flux Φ. The horizontal axis is the chemical potential. The colors represent the Chern numbers. The picture was made with the window condition equation (1.6) for $q = 512$ and p ranging in [1, 512]. The picture is apparently free from major coloring errors.

A numerical computation of the spectrum can be made efficiently for Hofstadter models that admit a 'Chambers relation' [6]: a relation that determines the points in the (magnetic) Brillouin zone where gap edges occur. To color figure 1, which has $q = O(550)$, one needs $O(10^5)$ Chern numbers. It is impractical to compute this many integers from their definition as integrals, equation (C.3). One needs a shortcut.

In the case of rational flux through the unit cell

$$\Phi = 2\pi p/q, \quad p, q \in \mathbb{N},\ gcd(p, q) = 1 \tag{1.1}$$

the Chern number of the jth gap, $\sigma_j \in \mathbb{Z}$, satisfies the Diophantine equation:

$$\sigma_j = sj \mod q, \tag{1.2}$$

s is the modular inverse of p, i.e. $sp = 1 \mod q$. The gap indexes j and s take values in $\mathbb{Z}_q$ assuming that all the gaps are open. The equation was first derived by a perturbation argument for the rectangular model in [18]. It was later shown to be a general result that holds for any periodic Schrödinger equation [9]. In appendix D we give a proof for tight-binding models.

The Diophantine equation forces distinct gaps to have different Chern numbers but leaves a mod q ambiguity in σ_j for $j \neq 0$. For $j = 0$ and $j = q$, corresponding to the semi-infinite gaps below and above the spectrum, there is, of course, no ambiguity: $\sigma_0 = \sigma_q = 0$: a trivial insulator [4].

The mod q ambiguity was resolved for the Hofstadter model on the rectangular lattice with nearest neighbors hopping in [18]. They showed, subject to the assumption that no gap opens or closes as the ratio of the horizontal to vertical hopping amplitudes changes away from zero, that σ lies in a window:

$$\sigma \in \begin{cases} \left[1-\frac{q}{2}, \frac{q}{2}-1\right] & q \text{ even;} \\ \left[-\frac{q-1}{2}, \frac{q-1}{2}\right] & q \text{ odd.} \end{cases} \tag{1.3}$$

When q is odd the window assigns q values to the Chern numbers but when q is even it only assigns $q-1$ values. This is still ok since the middle gap at $q/2$ (zero energy) is permanently closed in the rectangular model. The assumption that no gap closes upon the special deformation of the rectangular model used in [18] was subsequently proved in [7, 16]. This may be phrased as the statement that the Hofstadter models on the square and rectangular lattices are adiabatically connected.

For models, on other lattices, such as the Hofstadter model on the triangular lattice [2], or on the hexagonal lattice [8, 14], and models with hopping beyond nearest neighbors, the Diophantine equation still holds, but the issue of the mod q ambiguity is open. In all these models the mod q ambiguity is a *finite ambiguity* since the Chern numbers can be bounded in terms of the gap, see equation (C.6) in appendix C. However, the bound is not good enough to determine σ uniquely. A colored Hofstadter butterfly for the hexagonal model has been made in [11] where the Chern numbers were numerically computed using edge currents. This approach is numerically intensive.

The triangular and hexagonal lattices can be viewed as deformations of the square lattice by tuning the hopping amplitudes. For example, tuning the next nearest neighbor hopping amplitude along the north-west south-east bonds away from zero turns the square lattice to the triangular lattice. Two models are adiabatically connected if one can be deformed to the other without closing any gap implying that the resolution of the mod q ambiguity in the two models is the same. However, there is normally no way of telling *a priori* if all gaps remain open. In fact, by the Wigner–von Neumann crossing rule, [10], one would expect that generic deformations would open and close some gaps[4].

The Hofstadter model on the square lattice is not generic since its middle gap is closed for all even q. A generic Hofstadter model, though we cannot put our hands on one, should have all its gaps open.

One might think that one should be able to determine the Chern number easily from the Streda formula [17]

$$2\pi\delta\rho = \sigma\delta\Phi, \quad \rho = \frac{j}{q}. \tag{1.4}$$

The Streda formula, however, comes with a catch: it requires that one knows *a priori* that two neighboring points (ρ_1, Φ_1) and (ρ_2, Φ_2) belong to the same wing of the butterfly. Although humans can usually correctly guess when two points belong to the same wing, it is an intuition that is difficult to translate to an algorithm that would allow a computer to make this guess. Once the resolution reduces to the level of a single pixel, even humans cannot guess.

In this work we outline a graphic method to identify topological obstructions to adiabatic deformations which builds on the ability of humans to solve CAPTCHA (an acronym for *completely automated public Turing test to tell computers and humans apart*), which in this case translates to recognizing a coloring error.

We illustrate the method for the Hofstadter models on the triangular lattice [13]. In a triangular lattice there is a freedom to tune the fluxes in the up and down triangles, (Φ_u, Φ_d).

[4] A generic deformation of Hofstadter models is associated with a three-parameter family: two parameters for the Bloch momenta and one for the deformation.

Figure 2. The figure shows a coloring mistake for the pair ($p = 2, q = 5$): a blue streak at the center of the figure, representing $\sigma = -2$, cuts the wing $\sigma = 3$. The mistake reflects a wrong resolution of the mod q ambiguity of the solutions to the Diophantine equation.

This freedom allows for making various plots of infinitely many different butterflies. We have chosen to consider the case where the vertical axis in figure 1 is the total flux $\Phi_u + \Phi_d$ and $\Phi_d = \pi/2$ is fixed. We picked this particular value for Φ_d because it gives the butterfly inversion symmetry. It lacks the reflection symmetry of the rectangular and hexagonal lattices.

The Diophantine equation can be read as an assignment of a gap index j to a given Chern number. The resolution of the ambiguity for a gap index is obvious, since $j \in 1, \ldots, q$. The ambiguity problem for σ is now hidden in the fact that we do not know if a given σ, (rather than $\sigma \bmod q$) actually occurs. We know that $\sigma = 0$ occurs. This suggests the heuristics that small Chern numbers $|\sigma| \ll q$ occur. This is equivalent to saying that equation (1.3) holds for $|\sigma| \ll q$ and fails for $|\sigma| = O(q)$. An argument in favor of this heuristics can be made if one thinks of the Chern number as edge modes [4]. Generically, one expects edge modes to gap out so that their number is small.

Assuming this heuristics, the Diophantine equation can be written graphically as

$$\sigma_0 = 0 \rightarrow \sigma_p = 1 \rightarrow \cdots \leftarrow \ldots \sigma_{q-p} = -1 \leftarrow \sigma_q = 0 \tag{1.5}$$

which resolves the ambiguity for small Chern numbers $|\sigma| \ll q$. When the Chern numbers are $O(q)$, the assignment from the left and right in equation (1.5) disagrees reflecting the mod q ambiguity.

Figure 1, for the triangular lattice with $\Phi_d = \pm\pi/2$, was plotted assuming the shifted window condition

$$\sigma \in \left[-\frac{q}{2} + 1, \frac{q}{2}\right], q \text{ even}. \tag{1.6}$$

The window appears to be free from *major* coloring errors. On the scale of few pixels, it becomes difficult to tell if the coloring is indeed right. The points $(q \pm 1)/(2, q)$ were excluded because they lead to coloring errors illustrated in figure 2.

We have also numerically computed the Chern numbers, equation (C.3), for a few pairs (p, q) with small q and found:

$$\sigma \in \begin{cases} [\cancel{-1}, 0, 1],\ \text{gap closes} & q = 3,\ p \in \{1, 2\} \\ [\cancel{-2}, -1, \ldots, 3] & q = 5,\ p \in \{2, 3\} \\ \{-4, \cancel{-3}, -2, \ldots, 2, \cancel{3}, 4\} & q = 7,\ p \in \{3, 4\} \\ \{-4, \cancel{-3}, -2, \ldots 4, \cancel{5}, 6\} & q = 9,\ p \in \{4, 5\} \\ \{-8, \cancel{-7}, -6, \cancel{-5}, -4, \ldots, 4, \cancel{5}, 6, \cancel{7}, 8\} & q = 13,\ p \in \{5, 6\}. \end{cases} \tag{1.7}$$

This shows that there are pairs (p, q) for which the Chern numbers *do not* lie in any contiguous window.

There are topological obstructions for deforming the Hofstadter models on the triangular lattice with $\Phi_d = \pm\pi/2$ to the square lattice: the two models are not adiabatically connected. This is true even if one restricts oneself to odd q where all the gaps in the square model are open: the windows in equation (1.3) are incompatible with equations (1.6) and (1.7). Most (p, q) have gaps that must close. For example, the fragmented window $q = 7$, results from a deformation of the contiguous window $[-3, 3]$ upon gap closure taking $\pm 3 \mapsto \mp 4$.

Our findings, equations (1.6), (1.7), are consistent with the following conjecture:

Conjecture 1.1. *The mod q ambiguity in the solution of equation (1.2) is, for generic Hofstadter models, a sign ambiguity: the Chern number is either the smallest positive or the smallest negative solution of the Diophantine equation. Equivalently:* $-q \leqslant \sigma \leqslant q$.

The conjecture is related to an interesting separate problem namely, how to determine the sign of Chern numbers. Determining the sign of an integral is, of course, a much easier problem than evaluating it and can be estimated, with high probability using Monte Carlo methods. In fact, for small gaps, the sign of the Chern number is likely to be the sign of the curvature at the gap edged. If the conjecture was true, it would allow for efficient algorithms for plotting high resolution Hofstadter butterflies when the resolution of the mod q ambiguity is not known.

In the appendices we collect the tools we have used in the analysis.

Acknowledgments

The research was supported by ISF. JEA thanks Chris Marx, I Dana, G M Graf and O Zilberberg for useful discussions.

Appendix A. Hofstadter models on the triangular lattice

Define *magnetic hopping* $T_{1,2,3}$ on the triangular lattice,

$$(T_1\psi)(n, m) = \Psi(n, m-1),\ (T_2\Psi)(n, m) = \omega^m\Psi(n-1, m),\ T_3 = \omega_u T_1 T_2. \qquad \text{(A.1)}$$

See figure A1 for the meaning of ω, ω_d, and the coordinates (n, m). The unitary accumulated by going (clockwise) around the up/down triangles is $\omega_{u/d}$ and around the unit cell $\omega = \omega_u\omega_d$:

$$T_3^* T_2 T_1 = \omega_d, \quad T_3 T_2^* T_1^* = \omega_u, \quad T_2 T_1 = \omega T_1 T_2.$$

A (tight-binding) Hofstadter model with isotropic hopping amplitudes is

$$H(\omega, \omega_d) = T_1 + T_2 + T_3 + \text{h.c.} \qquad \text{(A.2)}$$

A.1. $\Phi_d = \pi/2$*: inversion symmetry*

Hofstadter models on the triangular lattice give the freedom to choose independently the fluxes in the up and down triangles. We have used this freedom to pick a model which is nice and symmetric.

The anti-unitary

$$C\Psi(n, m) = (-)^{m+n}\bar{\Psi}(n, m)$$

acts on $H(\omega, \omega_d)$ by

$$CH(\omega, \omega_d) = -H(\bar{\omega}, -\bar{\omega}_d)C. \qquad \text{(A.3)}$$

In a Hofstadter butterfly one looks at the spectrum as a function of the total flux Φ. It follows that $\omega_d = \pm i$ corresponds to a butterfly with inversion symmetry of the two axes of the diagram: $(\Phi, E) \leftrightarrow (-\Phi, -E)$, a symmetry evident in figure 1.

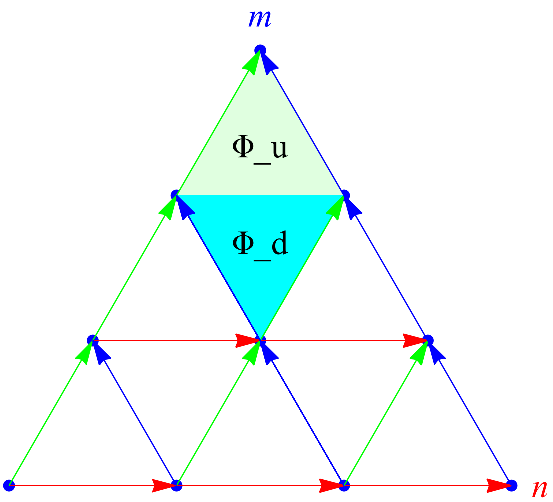

Figure A1. Triangular lattice. The flux through the down triangle is $e^{i\Phi_d} = \omega_d$, and the total flux through both up and down triangles is $\omega = e^{i\Phi}$. The coordinate n grows towards the right and the coordinate m grows towards the north-west. (n, m) is as in equation (A.1).

A.2. Reduction to one dimension

The operators T_j of equation (A.1) are independent of the coordinate n. The symmetry allows reducing the problem from two dimensions, $\mathbb{Z}^2$, to one dimension, $\mathbb{Z}$. Let T and S act on the one-dimensional lattice by

$$(T\psi)(m) = \psi(m-1), \quad (S\psi)(m) = \omega^m \psi(m), \quad ST = \omega TS. \tag{A.4}$$

Take $\Psi(n, m) = e^{-ik_1 n}\psi(m)$ labeled by the conserved (quasi) momentum $-\pi \leqslant k_1 \leqslant \pi$. One readily verifies that the action of T_j on such functions takes the form

$$T_1 \mapsto T, \quad T_2 \mapsto e^{ik_1} S, \quad T_3 \mapsto \omega_u e^{ik_1} TS.$$

The Hofstadter Hamiltonian on $\mathbb{Z}^2$ has been reduced to a periodic family of Hamiltonians, labeled by k_1, acting on $\mathbb{Z}$:

$$H(k_1) = T(\mathbb{1} + e^{ik_1}\omega_u S) + e^{ik_1} S + \text{h.c.}, \quad |k_1| \leqslant \pi. \tag{A.5}$$

A.3. Reduction to $q \times q$ matrices

T generates translations and since it commutes with itself it is translation invariant. S is not. However, when $\omega = e^{2\pi i p/q}$, a rational root of unity, $S^q = \mathbb{1}$. $H(k_1)$ is then periodic with period q. This allows the reduction of the operator $H(k_1)$ acting on $\ell^2(\mathbb{Z})$ to a $q \times q$ matrix $H(k_1, k_2)$ parametrized by two quasi-momenta $\mathbf{k} = (k_1, k_2)$.

Let S and T be the mod q version of equation (A.4)

$$S = \begin{pmatrix} \omega & 0 & \dots & 0 & 0 \\ 0 & \omega^2 & 0 & \dots & 0 \\ \dots & & \dots & \dots & \\ 0 & 0 & 0 & \omega^{q-1} & 0 \\ 0 & 0 & 0 & 0 & \omega^q \end{pmatrix}, \quad T = \begin{pmatrix} 0 & 0 & 0 & \dots & 1 \\ 1 & 0 & 0 & \dots & 0 \\ \dots & \dots & \dots & \dots & \dots \\ 0 & 0 & 1 & 0 & 0 \\ 0 & 0 & 0 & 1 & 0 \end{pmatrix}. \tag{A.6}$$

The $q \times q$ matrix obtained from equation (A.5) is

$$H(\mathbf{k}) = \mathrm{e}^{\mathrm{i}k_2} T(\mathbb{1} + \omega_u \mathrm{e}^{\mathrm{i}k_1} S) + \mathrm{e}^{\mathrm{i}k_1} S + \mathrm{h.c.} \tag{A.7}$$

The Bloch momenta $\mathbf{k}$ values takes in the (magnetic) Brillouin zone [19]

$$\mathrm{BZ} = \{\mathbf{k} | |k_1| \leqslant \pi, \ |qk_2| \leqslant \pi\}. \tag{A.8}$$

The matrices S and T satisfy the algebra

$$ST = \omega\, TS \quad S^q = T^q = \mathbb{1}. \tag{A.9}$$

A.4. Magnetic symmetry

The matrix $H(k_1, k_2)$ is *not* a periodic function on the (magnetic) BZ. However, it is periodic up to a unitary transformation. In fact, there is a larger symmetry, known as 'magnetic symmetry' [19].

The commutation of S and T, equation (A.9), implies

$$H(k_1, k_2) = T^* H\left(k_1 - \frac{2\pi p}{q}, k_2\right) T = S^* H\left(k_1, k_2 + \frac{2\pi p}{q}\right) S. \tag{A.10}$$

Since $gcd(p, q) = 1$, p has a modular inverse which we denote by s. Iterating equation (A.10) s times gives

$$H(k_1, k_2) = T^{s*} H\left(k_1 - \frac{2\pi}{q}, k_2\right) T^s = S^{s*} H\left(k_1, k_2 + \frac{2\pi p}{q}\right) S^s. \tag{A.11}$$

It follows that the spectral properties are fully determined by a small square in the BZ, Ω_H, whose size is $2\pi/q \times 2\pi/q$.

Appendix B. The Chambers relation and band edges

An efficient computation of the spectrum of Hofstadter models can be made provided there is *a priori* knowledge where in the BZ band edges occur. There is no known method to do that for general Hofstadter models, but Hofstadter models associated with tri-diagonal matrices are special. They admit the Chambers relation [2, 6, 12] which facilitates this. The Chambers formula says that characteristic polynomial takes the form

$$\det(H(\mathbf{k}) - \lambda) = P(\lambda) + \det H(\mathbf{k}) \tag{B.1}$$

$P(\lambda)$ is a polynomial in λ of degree q which is independent of $\mathbf{k}$. This says that for all p and q, band edges occur at the extremal points of $\det H(\mathbf{k})$.

For the triangular lattice with different fluxes in the up/down triangles [2] determined $\det H(\mathbf{k})$:

$$\det H(\mathbf{k}) = h(\omega, \omega_d) + (-)^{q+1}(\mathrm{e}^{\mathrm{i}qk_1} + \mathrm{e}^{\mathrm{i}qk_2} + (-)^{q-1}\bar{\omega}_d^q \mathrm{e}^{\mathrm{i}q(k_1+k_2)} + \mathrm{c.c.}). \tag{B.2}$$

B.1. Band edges for $\Phi_d = \pi/2$

For $\omega_d = i$ the extremal points of equation (B.2) are determined by:

(1) q odd: the maximum and minimum of

$$2(\cos x + \cos y \pm \sin(x + y)), \quad (x, y) = q\mathbf{k}. \tag{B.3}$$

The band edges occur at

$$\pm\, q\mathbf{k} \in (\pi/6, \pi/6), (5\pi/6, 5\pi/6). \tag{B.4}$$

(2) q even: the maximum and minimum of

$$2(\cos x + \cos y \pm \cos(x+y)), \quad (x, y) = q\mathbf{k}. \tag{B.5}$$

The band edges occur at

$$\pm\, q\mathbf{k} = (0, 0), (2\pi/3, 2\pi/3). \tag{B.6}$$

Appendix C. Chern numbers

The adiabatic curvature of the nth band is defined as [5]

$$\Omega_n(\mathbf{k}) = 2\ \mathrm{Im}\ \langle\partial_1\psi_n|\partial_2\psi_n\rangle = 2\ \mathrm{Im}\sum_{m\neq n}\frac{\langle\psi_m|\partial_1 H|\psi_n\rangle\langle\psi_n|\partial_2 H|\psi_m\rangle}{(E_n - E_m)^2}. \tag{C.1}$$

The Chern number $\tilde{\sigma}_n$ associated with the nth *band* is defined by [18]

$$\tilde{\sigma}_j = \frac{1}{2\pi}\int_{BZ}\Omega_n(\mathbf{k})\ \mathrm{d}^2k \in \mathbb{Z}. \tag{C.2}$$

The integration is over the (magnetic) Brillouin zone. It is known to be an integer [18]. Using the magnetic symmetry, section A.4, it can be written as [18]

$$\tilde{\sigma}_j = \frac{q}{2\pi}\int_{BZ/q}\Omega_n(\mathbf{k})\ \mathrm{d}^2k = \frac{q}{2\pi\mathrm{i}}\oint_{\partial(BZ/q)}\langle\psi_j|\nabla_k\psi_j\rangle\cdot\mathrm{d}\mathbf{k} \tag{C.3}$$

by the Stokes formula.

C.1. Chern numbers for gaps

The Chern number σ_j for the jth gap is defined as the sum of Chern numbers of the bands below the gap:

$$\sigma_j = \sum_{n\leqslant j}\tilde{\sigma}_n. \tag{C.4}$$

The summand in equation (C.1) is anti-symmetric under $m \leftrightarrow n$. It follows that

$$\sum_{n\leqslant j}\Omega_n(\mathbf{k}) = 2\,Im\sum_{n\leqslant j<m}\frac{\langle\psi_m|\partial_1 H|\psi_n\rangle\langle\psi_n|\partial_2 H|\psi_m\rangle}{(E_n - E_m)^2}. \tag{C.5}$$

In the Hofstadter model, equation (A.7), $\partial_j H$ is a sum of six unitary operators and so $\|\partial_j H\| \leqslant 6$. It follows that with g_j the gap

$$\left|\sum_{n\leqslant j}\Omega_n(\mathbf{k})\right| \leqslant \frac{2\times 6^2}{g_j^2}\sum_{n\leqslant j<m}1 = \frac{2\times 6^2 j(q-j)}{g_j^2}.$$

The area of BZ is $(2\pi)^2/q$ and hence

$$|\sigma_j| \leqslant \frac{4\pi\times 6^2 j(q-j)}{q\ g_j^2}. \tag{C.6}$$

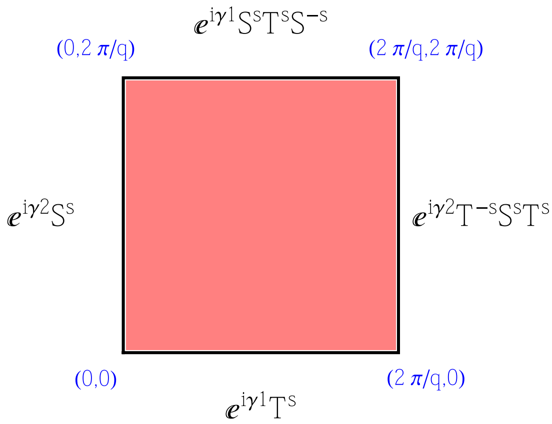

Figure D1. The unitaries that relate $|\psi\rangle$ at the corners of the square $2\pi/q \times 2\pi/q$ by parallel transport along the corresponding edges.

Appendix D. Diophantine equation

The nth band is associated with a projection $P_n(\mathbf{k}) = |\psi_n\rangle\langle\psi_n|$. We shall suppress n to simplify the notation. P is determined by the Hamiltonian and inherits its symmetries. In particular, $P(\mathbf{k})$ is periodic, with period $2\pi/q$, up to the unitaries T^s and S^s as per equation (A.11).

The Chern number of the nth band is, by equation (C.3), $q/2\pi$ times the holonomy in the phase of $|\psi\rangle$ as one parallel transports the state around the square

$$(0,0) \to (2\pi/q, 0) \to (2\pi/q, 2\pi/q) \to (0, 2\pi/q) \to (0,0).$$

A parallel transport that keeps Berry's phase, without accumulating a 'dynamical phase' is given by the solution of the differential equation [15]

$$|\mathrm{d}\psi\rangle = \mathrm{i}[\mathrm{d}P, P]|\psi\rangle. \tag{D.1}$$

This evolution equation guarantees that $|\psi\rangle$ stays in range P, i.e. $P|\psi\rangle = |\psi\rangle$ all along the path: it satisfies the adiabatic theorem with no error.

Let $|\psi\rangle_{(2\pi/q,0)}$ be the solution of equation (D.1) along the open path $(0,0) \to (2\pi/q, 0)$. This defines a phase γ_1 by

$$|\psi\rangle_{(2\pi/q,0)} = \mathrm{e}^{\mathrm{i}\gamma_1} T^s |\psi\rangle_{(0,0)}. \tag{D.2}$$

Similarly, let $|\psi\rangle_{(0,2\pi/q)}$ be the solution of equation (D.1) along the path $(0,0) \to (0, 2\pi/q)$. It defines a phase γ_2 by

$$|\psi\rangle_{(0,2\pi/q)} = \mathrm{e}^{\mathrm{i}\gamma_2} S^s |\psi\rangle_{(0,0)}. \tag{D.3}$$

Now, we can get two different determinations of $|\psi\rangle_{(2\pi/q,2\pi/q)}$, one along the path $(0,0) \to (2\pi/q, 0) \to (2\pi/q, 2\pi/q)$ and the other along the path $(0,0) \to (0, 2\pi/q) \to (2\pi/q, 2\pi/q)$. The discrepancy in the phases is the holonomy in phase associated with going around the square. This phase is precisely the value of the integral in equation (C.3), which we are after.

By the magnetic symmetry, equation (A.11), parallel transport along the path $(2\pi/q) \to (2\pi/q, 2\pi/q)$ assigns the phase (see figure D1)

$$|\psi\rangle_{(2\pi/q,2\pi/q)} = \mathrm{e}^{\mathrm{i}\gamma_1} S^s T^s S^{-s} |\psi\rangle_{(0,2\pi/q)}. \tag{D.4}$$

Similarly, parallel transport along the path $(2\pi/q, 0) \rightarrow (2\pi/q, 2\pi/q)$ assigns a different phase to the same state

$$|\tilde{\psi}\rangle_{(2\pi/q,2\pi/q)} = \mathrm{e}^{\mathrm{i}\gamma_2} T^{-s} S^s T^s |\psi\rangle_{(2\pi/q,0)}. \tag{D.5}$$

Inserting equations (D.2) and (D.3) in equations (D.4) and (D.5) we find that the disagreement (holonomy) between these two assignments is

$$S^{-s} T^{-s} S^s T^s = (\omega^s)^s = \mathrm{e}^{2\pi \mathrm{i} s/q}. \tag{D.6}$$

It follows from this and equation (C.3) that the Chern number of a single non-degenerate band j satisfies the Diophantine equation:

$$\sigma_j = s \mod q.$$

This completes the proof of the Diophantine equation.

References

[1] Avron J E, Osadchy D and Seiler R 2003 A topological look at the quantum Hall effect *Phys. Today* **56** 38–42
[2] Bellissard J, Kreft C and Seiler R 1991 Analysis of the spectrum of a particle on a triangular lattice with two magnetic fluxes by algebraic and numerical methods *J. Phys. A: Math. Gen.* **24** 2329
[3] Bellissard J and Simon B 1982 Cantor spectrum for the almost Mathieu equation *J. Funct. Anal.* **48** 408–19
[4] Bernevig B A and Hughes T L 2013 *Topological Insulators and Topological Superconductors* (Princeton, NJ: Princeton University Press)
[5] Berry M V 1984 Quantal phase factors accompanying adiabatic changes *Proc. R. Soc.* A **392** 45–57
[6] Chambers W G 1965 Linear-network model for magnetic breakdown in two dimensions *Phys. Rev.* **140** A135–43
[7] Choi M-D, Elliott G A and Yui N 1990 Gauss polynomials and the rotation algebra *Inventiones Math.* **99** 225–46
[8] Claro F H and Wannier G H 1979 Magnetic subband structure of electrons in hexagonal lattices *Phys. Rev.* B **19** 6068–74
[9] Dana I, Avron Y and Zak J 1985 Quantised Hall conductance in a perfect crystal *J. Phys. C: Solid State Phys.* **18** L679
[10] Friedland S, Robbin J W and Sylvester J H 1984 On the crossing rule *Commun. Pure Appl. Math.* **37** 19–37
[11] Agazzi A, Eckmann J-P and Graf G M 2014 The colored Hofstadter butterfly for the honeycomb lattice (http://xxx.lanl.gov/abs/1403.1270v1)
[12] Han J H, Thouless D J, Hiramoto H and Kohmoto M 1994 Critical and bicritical properties of Harper's equation with next-nearest-neighbor coupling *Phys. Rev.* B **50** 11365–80
[13] Hatsugai Y and Kohmoto M 1990 Energy spectrum and the quantum Hall effect on the square lattice with next-nearest-neighbor hopping *Phys. Rev.* B **42** 8282–94
[14] Hatsugai Y, Fukui T and Aoki H 2006 Topological analysis of the quantum Hall effect in graphene: Dirac–Fermi transition across van Hove singularities and edge versus bulk quantum numbers *Phys. Rev.* B **74** 205414
[15] Kato T 1950 On the adiabatic theorem of quantum mechanics *J. Phys. Soc. Japan* **5** 435–9
[16] Mouche P v 1989 The coexistence problem for the discrete Mathieu operator *Commun. Math. Phys.* **122** 23–33
[17] Streda P 1982 Theory of quantised Hall conductivity in two dimensions *J. Phys. C: Solid State Phys.* **15** L717
[18] Thouless D J, Kohmoto M, Nightingale M P and den Nijs M 1982 Quantized Hall conductance in a two-dimensional periodic potential *Phys. Rev. Lett.* **49** 405–8
[19] Zak J 1964 Magnetic translation group *Phys. Rev.* **134** 1602–6